Influence of nuclear dynamics on neutron scattering from ^{194}Pt

S. E. Hicks, J. P. Delaroche,* M. C. Mirzaa,† J. Hanly, and M. T. McEllistrem
Department of Physics and Astronomy, The University of Kentucky, Lexington, Kentucky 40506
(Received 27 January 1987)

Measurements of neutron differential scattering cross sections at 4.55 MeV, and of neutron total cross sections at low energies have been made with an isotopically enriched sample of ^{194}Pt. These results are combined with earlier neutron scattering data measured at 2.5 MeV in a consistent set of coupled channels analyses based on the low-lying collective excitations of ^{194}Pt. The results of these measurements and analyses extend the tests of the collective character of ^{194}Pt, and show the strong relationship between scattering and the dynamics of nuclear excitations. We are able to discriminate amongst different models which have been offered to interpret the low-lying structure of this nucleus. Some information from an associated 8 MeV neutron scattering experiment is also included; the entire neutron data set allows us to determine that the strength of the real scattering potential has a nonlinear neutron energy dependence, and further that its geometry must be energy dependent.

I. INTRODUCTION

Recent studies of neutron scattering from heavy collective nuclei,[1,2] have been designed to probe the extent to which the effects of different collective excitations can be separately determined for each collective level, particularly for those levels which are not the most strongly excited ones. As noted in earlier studies[1,2] the very strong coupling to quasi-ground-state band, or to one phonon vibrational excitations, has been an important source of information about those excitations.[3,4] The sensitivity of neutron scattering observables to excitations other than these strongest inelastic excitations is not clear. There is also the point that for some nuclei neutrons may provide excitation strengths different from those deduced with other probes.[4,5] That seems to be the case for ^{194}Pt, yielding valuable constraints on the roles played by target neutrons and protons. The question of excitation strengths found in scattering with different hadrons is explored most directly in another report.[6]

The usefulness of working in the Os and Pt regions when testing sensitivity to non-ground-state band excitations was mentioned in an earlier study[2] of ^{194}Pt. The γ-band excitation strengths and collective character vary rapidly through this set of nuclei.[2,7] The present report extends the study of excitations in ^{194}Pt first presented in Ref. 2, and other reports will present results for other nuclei of this mass region. In Ref. 2 differential elastic and inelastic scattering cross sections at a neutron energy $E_n=2.5$ MeV and limited information from total cross sections had provided tests of several structure models. Total cross sections had been available[8] for energies between 1.8 and 20 MeV, but only for natural abundance Pt, and with rather large uncertainties. Additional total cross section data exist from a much older data set, which extended total cross sections to nearly 30 MeV.[9]

The earlier study of Pt nuclear structure effects on neutron scattering, Ref. 2, showed that γ-unstable models, such as the interacting boson approximation (IBA) near the O(6) subgroup limit, or the dynamic deformation theory (DDT) of Kumar, gave results consistent with the cross sections while asymmetric rotor models (ARM's) did not. Indeed, there are at least half a dozen models interpreting the bound state structures in the Os–Pt region, all presenting interpretations in terms of varying degrees of γ softness, and several could describe those measurements within uncertainties.

In this work we present new measurements of neutron differential scattering cross sections and total cross sections, all measured with a sample of high isotopic enrichment[10] in ^{194}Pt. The total cross sections span the energy interval from 300 keV to 4 MeV, and the differential scattering cross sections are measured for $E_n=4.55$ MeV. Older studies[11] show that low energy total cross sections are especially sensitive for testing coupling between scattering channels. Analyses completed in this work show that the 4.55 MeV elastic scattering cross sections are particularly sensitive to the scattering geometry. They are also particularly sensitive to the strength of the real part of the optical potential, and to the couplings between scattering channels. These heightened sensitivities reflect the fact that 4.55 MeV is a low energy, where sensitivity to channel couplings is known[1,2] to be high; but the energy is still high enough that compound nucleus cross sections, which are structure insensitive, are negligible. Direct coupling between scattering channels is the only important reaction mechanism.

As in the previous study,[2] interpretation of these new data in terms of coupled channels models shows that only γ-unstable or γ-soft models could possibly describe the measurements. Further, even discrimination among the different γ-unstable and γ-soft models is now possible, particularly because of the new, accurate set of total cross sections. We show also that this new, sensitive interpretation of neutron scattering is completely consistent with the earlier data set;[2] in fact, we are now able to present a better description of the earlier data.

Finally, while the combined analyses of all of these data sets were being completed, a new experiment providing 8 MeV neutron scattering cross sections was in progress at

the Centre d'Etudes de Bruyères-le-Châtel[12] (BRC). Combining a little of the data from that extensive study with the data of Ref. 2 and the present measurements enables us to draw some surprising conclusions about the energy dependence of the scattering potential. We find that a nonlinear energy dependence of the real potential strength is required at low neutron energies and, further, that its scattering geometry must be energy dependent.

II. METHODS AND PROCEDURES

A. Experimental methods

While many new measurements are provided in this study, the focus of this report is on analysis and interpretation of scattering cross sections from several scattering experiments in terms of nuclear structure models. Hence the description of experimental methods will be brief. This is appropriate, since the experimental methods have been well detailed in previous publications from this laboratory.[2,3,13] The particular methods and geometry used for measurements of differential scattering cross sections with the rather small powdered metal sample of isotopically enriched ^{194}Pt were described and illustrated in Ref. 2. The 0.2 mol sample was mounted 8.4 cm from the center of a tritium (T) gas cell; the ^{3}H(p,n)^{3}He reaction was used as the source of the 4.55 MeV incident neutrons. The shielded neutron scintillation detector[2] was mounted 3.7 m from the sample for time-of-flight (TOF) separation of neutrons scattered to the different levels of ^{194}Pt. Scattering was observed to the first three members of the quasi-ground-state band and the 2_2^+ level. The total energy resolution of the neutron TOF spectra was approximately 110 keV.

The total cross section measurements required particular care, in order to avoid problems associated with normal position instabilities of the accelerator beam since the ^{194}Pt sample was quite small, a cylinder only 1.28 cm in diameter by 1.54 cm long, with a total ^{194}Pt mass of 40 g. For the total cross section measurements the ^{194}Pt cylindrical sample was mounted with its axis on that defined by the proton beam entering the tritium gas cell, and 1.5 m from the end of the cell. The neutron detector was centered in the main scattering shield illustrated in Fig. 1 of Ref. 2, and at a distance of 3 m from the tritium cell. Thus the sample was equidistant from the shielded detector and from the neutron source. For these measurements the detector was a 5 cm diam by 5 cm thick liquid NE218 scintillator. The mouth of the detector shield contained a brass collimator with a 2 cm diam aperture, to reduce entry of scattered neutrons into the shield and preserve good geometry. The neutron collimation system between source and sample included a "forced reflection" collimator of the type proposed by Spencer.[14] The collimator included 7.65 cm thick baffles of Cu and Pb, together with the two element forced reflection collimator of Li_2CO_3 loaded paraffin.[14] The entire collimator was about 1.5 m long; that is, it essentially filled the space between the neutron source and the samples. The collimation system has an effective aperture diameter of 0.8 cm, and the entire system is housed inside a 2.5 ton shield also made of Li_2CO_3 loaded paraffin. Components of the cylindrical system were aligned on the beam-defined axis to within 0.5 mm with a laser beam. A full description of the system and measurement procedures is contained in the dissertation of one of the authors.[15]

The largest problem with the total cross section data stemmed from position uncertainties of the proton beam in the T-gas cell. The beam is focused into the cell with a 90° Mobley bunching magnet, and current regulation for that magnet was discovered to be less than optimum during the experimental runs. Magnet current was thus monitored and corrected manually; residual errors made the most important contribution to uncertainties. In-scattering effects were calculated using the method described in Ref. 16. These corrections were found to be $\leq 0.1\%$ and were thus considered to be insignificant. Corrections were made for the effects of resonance or sample self-shielding;[17] these corrections were found to be negligible above 1 MeV incident neutron energy. Total uncertainties amounted to about 2% per point;[15] cross sections were verified by simultaneously measuring the total cross sections of carbon, which are known to better than 1% in the energy range of this experiment.

B. Analysis procedures

As in previous studies, low energy scattering properties,[2] such as strength functions and scattering lengths, were constraints in fixing the scattering potentials. In addition, we had the new total cross sections shown in Fig. 1. The measurements cover the energy range from 300 keV to 4 MeV. These data are very important in fixing the scattering potentials for different neutron energies. In the region of overlap of our separated isotope measurements and the natural sample measurements[8] of Poenitz *et al.*, the two data sets agree within experimental uncertainties. Hence the natural abundance, lower precision cross sections from Ref. 8, plotted in Fig. 2, and those of Ref. 9, were used to extend the potential determination up to 30 MeV. The greatest sensitivity to potential and structure model, however, is found in total cross sections from 300 keV to about 2.5 MeV, and in the elastic scattering cross sections at 4.55 MeV.

The procedure followed in calculating scattering cross sections included choosing a collective structure model which has been tailored to fit the level energies and electromagnetic transition rates of ^{194}Pt. The $E2$ and $E4$ matrix elements of that model, which represented the gamma-ray transitions between levels and $E2$ moments of bound levels, were then used to fix the relative coupling strengths between scattering channels. Six low-lying collective levels of ^{194}Pt were included in the coupled channels (CC) model space, the first three levels of both the ground state and γ bands. However, most CC calculations were done only with the five natural parity levels, since the 3^+ level affected other level calculations negligibly.

For a scattering analysis each structure model must be combined with a scattering potential whose parameters are varied to optimize the description of all scattering data within the context of that model. All CC analyses were

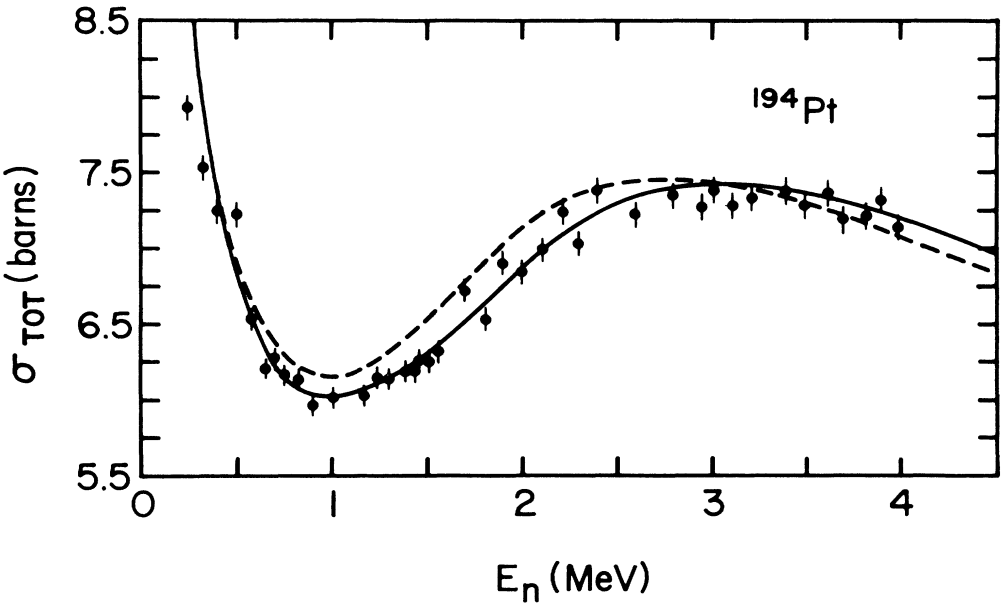

FIG. 1. Neutron total cross section data for ^{194}Pt along with two model calculations. The solid curve is from the DDT, while the dashed curve would be representative of either the ARM or IBA-2.

carried out using the computer code[18] ECIS79. Special handling routines had been developed here to use total cross sections as a function of neutron energy and differential elastic scattering cross sections as input information to automatic search routines of ECIS79. Scattering potential parameters were varied in multiparameter and single parameter searches to find the best representation possible within the context of the particular structure model chosen to represent the bound levels of ^{194}Pt. Decisions as to best fits were always made through visual inspection of calculated and measured cross sections, as well as noting chi-square values from the search procedures. Although compound system (CS) cross sections were almost negligible for these purposes, no more than about 0.5 mb/sr for any single level at an incident neutron energy of 4.55 MeV, they were carefully calculated and included using models and procedures described[2] earlier. These calculations are accurate to about 10%, which means uncertainties in them are insignificant as regards the present coupled channels models tests.

III. NEUTRON SCATTERING: RESULTS AND INTERPRETATIONS

The measured total cross sections and some model calculations are shown in Figs. 1 and 2. The points in Fig. 1 are measured with the sample enriched to 96% in ^{194}Pt; total uncertainties are indicated. The points of Fig. 2 are from recent measurements[8] using natural abundance Pt. Since our new measurements of Fig. 1 extend to 4 MeV, we have useful total cross sections up to 30 MeV incident energy, with the proviso that above 4 MeV the data are only for natural Pt. The natural abundance cross sections of Poenitz *et al.*[8] are in good agreement with the present results of Fig. 1 for ^{194}Pt. The solid curve shown in Fig. 2 is an extension of any of the model calculations which provide a good fit to the data of Fig. 1. As expected, these total cross sections tell us a great deal about the applicability of different models. An unexpected finding is that these data also serve to provide important constraints on the energy dependence of scattering potential parameters, to be discussed later.

The elastic scattering differential cross sections for an incident neutron energy of 4.55 MeV are shown in Fig. 3 with calculations of three models. Two of them gave results too similar to each other to separate in Fig. 3. The model tests are discussed separately below. Several of the models are sufficiently similar that the potentials needed with them are also rather similar; others require distinct potentials. As noted earlier, the different nuclear structure models are characterized, for present analytical purposes, by the sets of $E2$ and $E4$ matrix elements which connect levels of the target nuclei to each other through gamma-ray transitions. The interacting boson approximation with separate boson parameters for protons and neutrons[19,20] (IBA-2), and Kumar's dynamic deformation theory[21] (DDT) provide $E2$ matrix elements which are quite similar to each other for ^{194}Pt. The matrix elements for these and several other models are listed in Table I. It is not surprising that different models provide similar $E2$ matrix elements, since all provide reasonable descriptions of level energies and gamma-ray spectra of the same nucleus. Finally, there is a set of $E2$ matrix elements in Table I, labeled CE, which comes from model independent analyses of Coulomb excitation experiments performed with several different heavy ions.[22] Any of these models, or the CE results, can be tested in scattering. The model tests to be presented here are not very sensitive to the set of $E4$ matrix elements used. All of the model calculations included both $E2$ and $E4$ matrix elements, but most of the following discussion focuses on the sensitive $E2$ matrix elements.

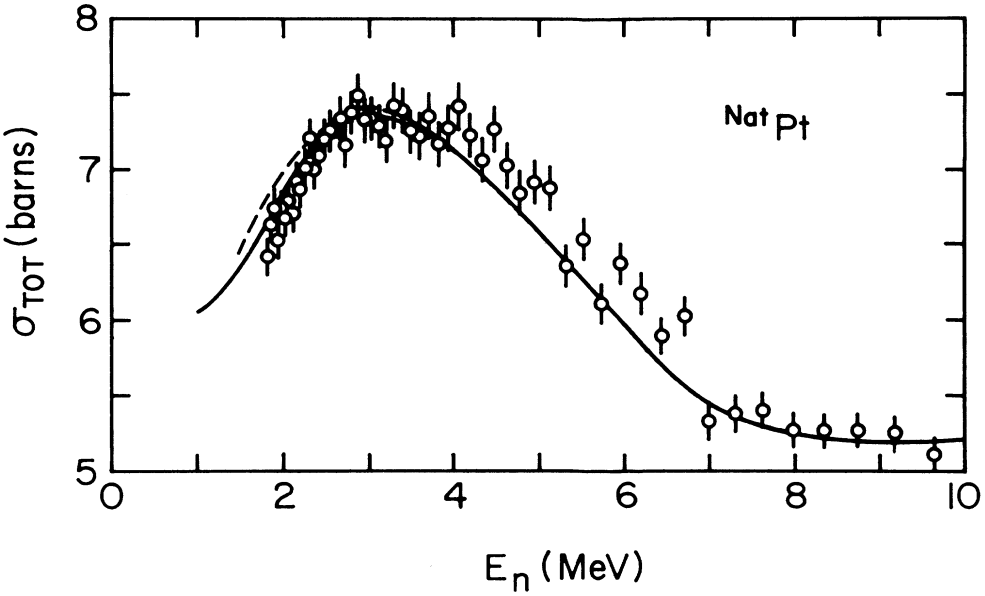

FIG. 2. Neutron total cross sections for natural Pt taken from Ref. 8. The solid curve is representative of any of the better models discussed, i.e., DDT, IBA-1, or γ-soft. The dashed curve comes from the CE reduced matrix elements.

A. Asymmetric rotor model (ARM)

The ARM, fitted to transition rates and energy levels, had failed badly[2] to fit the elastic scattering differential cross sections at 2.5 MeV incident neutron energy. The new total cross section data of Fig. 1 constrain the scattering potential more than before, and the failure reported[2] at 2.5 MeV now becomes more pronounced. The best description of total cross sections achieved was that of the dashed curve of Fig. 1. The elastic scattering diffraction pattern is shifted forward of the scattering data of Fig. 3 of Ref. 2 noticeably more than shown there, where it was already forward of the measured pattern. In contrast, this same ARM leaves a calculated pattern shifted *behind* the elastic scattering data at 4.55 MeV, as shown by the dotted-dashed curve of our Fig. 3. The calculated total cross sections shown in Fig. 1 as the dashed curve are well above the data from 0.5 to 2.0 MeV. It is important to note that these three comparisons are the best that can be done after extensive searches on potential parameters. They are approximately insensitive to small changes in the coupling parameters β_2 or γ of the model. Wu and Cline[22] also have found that the ARM is quite inconsistent with their extensive Coulomb excitation results.

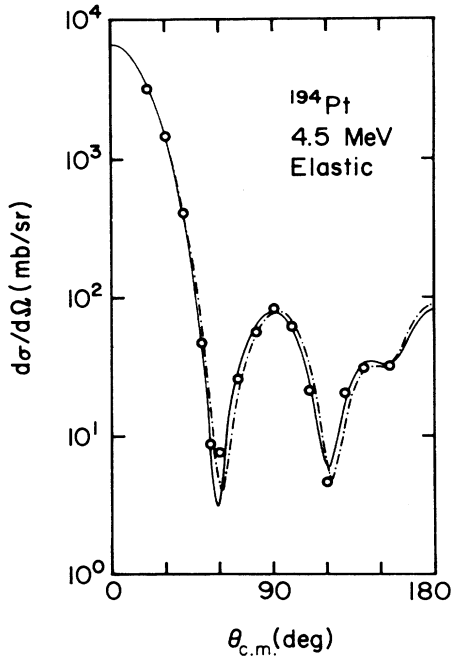

FIG. 3. Neutron elastic scattering differential cross sections from ^{194}Pt. The uncertainties would be smaller than the data points. The solid curve is from the DDT with altered 2_1^+ quadrupole moment as discussed in the text. The dotted-dashed curve is from the ARM. The IBA-2 model would give results very close to the solid curve.

B. IBA-2 and DDT models

Two IBA-2 descriptions have been developed for ^{194}Pt: an early version by Bijker and Dieperink[19] and a revision of that description three years later.[20] The earlier version[19] and the DDT model[21] have many similar $E2$ matrix elements, as shown in Table III of Ref. 2. Both models had been found adequate as descriptions of neutron scattering at 2.5 MeV.[2] Matrix elements of the DDT and the newer IBA-2 description[20] are presented in Table I; the newer IBA-2 model will be tested in the present analyses, although there are clear reasons to prefer the first form of the IBA-2 model to the newer one. First, the earlier[19] IBA-2 description contained the smallest quadrupole moment for the 2_1^+ level, most consistent with recent measurements.[23,24] Second, the sign of the very small $E2(0_1^+ \rightarrow 2_2^+)$ matrix element is correctly reproduced in the earlier version, but not in the newer version;[20] this

TABLE I. $E2$ matrix elements of several different models for levels and transition rates in ^{194}Pt. The acronyms heading different columns (for different models) are defined in the text. All levels are even parity.

				IBA-1			
J_i	J_f	CE	IBA-2	($\kappa=0.04$)	($\kappa=0.54$)	DDT	γ-soft
0_1	2_1	−1.0	−1.0	−1.0	−1.0	−1.0	−1.0
0_1	2_2	−0.074	−0.101	0.0046	0.063	0.053	0.0
2_1	2_1	−0.407	−0.54	−0.014	−0.196	−0.5	0.0
2_1	4_1	−1.614	−1.655	−1.551	−1.552	−1.672	−1.654
2_1	2_2	−1.255	−1.317	−1.156	−1.142	−1.145	−1.233
4_1	4_1	−0.764	−0.748	−0.013	−0.175	−0.67	0.0
2_2	2_2	0.415	0.498	0.014	0.196	0.43	0.0

sign is very important for fitting our total cross sections.

The total cross sections at low energy constrain the scattering potential, so that our present analyses with the new IBA-2 model[20] produce a chi-square value (χ^2) for the 2.5 MeV elastic scattering data which is at least twice the value found in Ref. 2, and also more than twice the value for the best models tested in the present analyses. The elastic scattering description of the IBA-2 model at 4.55 MeV (not shown) would be worse than the solid curve of Fig. 3. The first minimum is too deep, and the second too shallow. The total cross section calculation is represented by the dashed curve of Fig. 1, very similar to that of the ARM. As before, the potential parameters have already been adjusted to optimize the fit to the data of Figs. 1 and 3. Thus we see that the calculations for this IBA model fail about as badly, particularly for the total cross sections, as do those for the ARM. The inelastic scattering cross sections calculated and measured[2] at 2.5 MeV are shown in the left-hand panel of Fig. 4 as solid and dashed curves for the 2_1^+ and 2_2^+ levels, respectively. This is close to the calculations shown in Ref. 2, and they are low at forward angles. The failure of the total cross section calculations and the poor 4.55 MeV differential scattering calculations suggest that the revised IBA-2 model does not provide an adequate description of the nuclear dynamics of ^{194}Pt.

Calculations with the DDT model of Kumar[21] are the first to be presented here which provide a rather good description of the neutron scattering data at all energies. Calculations were done with the model as presented in Table I, and also with minor modifications made to it. Those to be shown include one slight modification to the

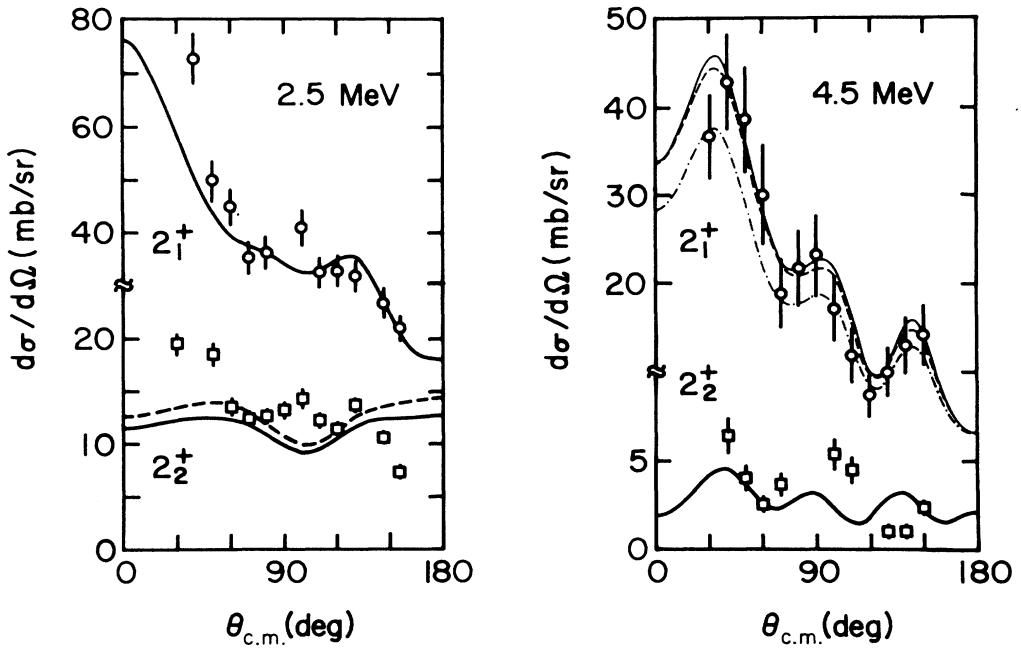

FIG. 4. Inelastic neutron scattering cross sections from the first two 2^+ levels at 2.5 and 4.55 MeV. The solid curves are all representative of the DDT, as modified to fit the experimental 2_1^+ quadrupole moment. The dashed curves are from the IBA-2 and are sometimes not distinguishable from the solid curves. The dotted-dashed curve is from the DDT using $\beta_2=-0.16$, as discussed in Sec. III F.

reorientation $E2$ matrix element of the 2_1^+ level. In all realistic models this element must be, and is, small, a result of the accidental cancellation of large contributions to the matrix element. The small value of Table I was replaced by an even smaller value, $M_2(E2; 2_1^+ \rightarrow 2_1^+) = -0.200$. This modest change puts the quadrupole moment of the first 2_1^+ level, $Q(2_1^+) = 0.18$ e b, in agreement with the most precise pair of measured values[23] of 0.14 ± 0.03 e b.

There are four recent measurements of the 2_1^+ quadrupole moment, three from reorientation terms in Coulomb excitation experiments[22–24] and one from μ-mesic atomic spectra.[25] The result of Chen *et al.*[23] comes from a careful reexamination of Coulomb excitation in ^{194}Pt, repeating an earlier, less accurate measurement. This result is in good agreement with the μ-mesic atom result,[25] whose interpretation has little model dependence. Two other Coulomb excitation experiments[22,24] yield $Q(2_1^+)$ values still small, but 2.5 times larger than the cited pair. Our neutron scattering analyses show a clear preference for the smaller average of the pair of results cited above, the value $Q(2_1^+) = 0.14$ e b. Adopting the revised reorientation matrix element is an insignificant model change, but has a marked effect on scattering cross sections, to be noted later.

The DDT fit to low energy total cross sections is shown as the solid curve of Fig. 1, an excellent result. This fit continues to 10 MeV, as shown with the solid curve of Fig. 2, and to 30 MeV in Fig. 5 of Ref. 2. Continuing the fit to 30 MeV is important to characterize properly the higher energy dependence of the scattering potential. The fit to the 2.5 MeV elastic scattering data[2] (not shown here) is good. The comparison at 4.55 MeV is shown in Fig. 3 as the solid curve. The problem of fitting in the minima is partially (although not entirely) alleviated. Calculations for the 2_1^+ level are shown in the right-hand panel of Fig. 4 at 4.55 MeV, again as the solid curve, providing an excellent description of the measurements. Also shown in Fig. 4, the dotted-dashed curve, is the result of lowering the quadrupole deformation amplitude, β_2, below its optimum value by 6%. This shows that $\beta_2 = -0.17 \pm 0.005$, quite sensitively determined. For all successful models tested this was found to be the optimum value, with about the same sensitivity. The value determined does reflect on the chosen scattering potential, which is very sensitively determined by the large set of neutron scattering data.

As noted above, many IBA-2 and DDT reduced matrix elements $M_2(E2)$ are similar, yet the models have quite different success, particularly for the total cross sections. For total cross sections the difference comes largely from the sign of the $E2(0_1^+ \rightarrow 2_2^+)$ matrix element, a very small matrix element indeed, and a very sensitive result of any model, but it is very important for low energy total cross sections. The DDT and other models clearly require that this matrix element must be positive, in our sign convention. Another $M_2(E2)$ examined was the 2_1^+ reorientation matrix element, discussed above. Altering $E2(2_1^+ \rightarrow 2_1^+)$ as indicated had no effect on total cross sections, but improved the elastic scattering calculations in the minima at 4.55 MeV, and increased the calculated inelastic scattering cross sections at small angles for the 2_1^+ level. These improvements are thus reflected in the solid curve of Fig. 3 and all curves of the right-hand panel of Fig. 4.

C. IBA-1 and gamma-soft models

The IBA-1 model very near the O(6) subgroup limit was the original model deployed[7] to give a remarkably successful description of energy levels and transition rates in ^{196}Pt. It was a substantial success partly because it gave us a new geometric picture, that of the γ-unstable vibrator, well related to spherical vibrators and deformed rotors. This picture was then applied, slightly modified,[26] as a description of ^{194}Pt. This modified IBA-1 model was used[26] by Deason *et al.* (PTD) to describe 35 MeV proton scattering to many levels of ^{194}Pt and other Pt nuclei. The form of the model Hamiltonian which was best suited for bound level properties had a very weak residual quadrupole-quadrupole coupling term to break the O(6) symmetry; the quadrupole coupling parameter $\kappa = 0.04$ implied very little deviation from the γ-unstable limit, and strong similarity to ^{196}Pt. A strong quadrupole-quadrupole interaction, breaking substantially the O(6) symmetry, would correspond to a value of κ near 0.5. In their 35 MeV proton scattering analyses PTD did find that such a larger value, $\kappa = 0.54$, was needed particularly for scattering to the 2_2^+ level. Matrix elements from both IBA-1 models are presented in Table I. Of course, using the larger value of κ diminishes the claim[7] that the heavier Pt nuclei are outstanding examples of an O(6) dynamical symmetry.

We had great difficulty with both IBA-1 model results in our earlier 2.5 MeV neutron scattering experiment, since they seemed to provide inelastic scattering cross sections to the 2_1^+ level which were much too low. Since that work we have discovered, through direct calculation of proton scattering, that the $E2$ matrix elements $E2(2_1^+ \rightarrow 4_1^+)$ were published with the wrong sign in both Deason's dissertation and in the subsequent paper (PTD).[26] That error has been corrected in Table I, and the IBA-1 model, either with $\kappa = 0.04$ or 0.54, gives a good description of both elastic and inelastic neutron scattering cross sections to the five low lying excited levels of our coupled channels model space, except that the inelastic scattering cross sections to the 2^+ levels are still a little low. The elastic scattering description with $\kappa = 0.04$ at 4.55 MeV is shown in Fig. 5 as the dashed curve. The fit is slightly worse when the model with $\kappa = 0.54$ is used, because the minima are shifted toward back angles. The inelastic scattering cross sections to the 2^+ levels are shown as solid curves in Fig. 6; for them there is no detectable difference between the two IBA-1 model results. Both provide excellent descriptions at 2.5 MeV incident energy except for the 2_2^+ level; all models introduced to this point provide cross sections too small compared to measured values for that level, and with angular distributions shifted with respect to the data.

The last model to be introduced is the γ-soft model of Leander,[22,27] as fixed to the level energies and electromagnetic transition rates of ^{194}Pt by Wu and Cline.[22] The cross sections provided by this model are just those of the solid curves of Figs. 5 and 6, except for that to the 2_2^+ lev-

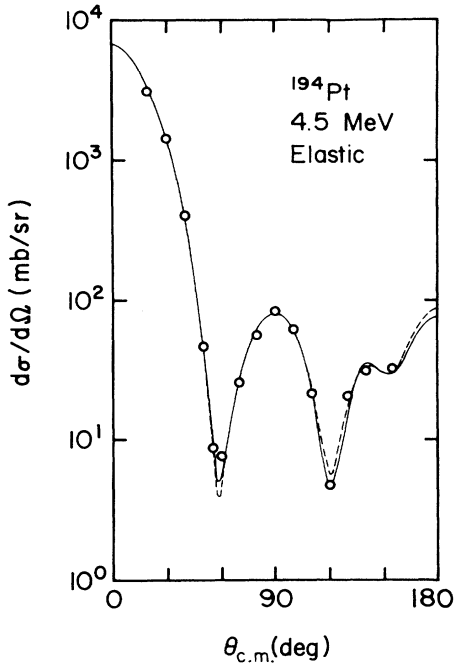

FIG. 5. The neutron elastic scattering cross section at 4.55 MeV; the solid and dashed curves are representative of the γ-soft and IBA-1 models, respectively.

el at 2.5 MeV incident energy. The dotted-dashed curve of Fig. 6 is obtained for that level from the γ-soft model, the best result from any model. The fits in Figs. 5 and 6 collectively are substantially better than those for the models represented in Figs. 3 and 4. The total cross sections of the γ-soft model are the solid curves of Figs. 2 and 7, also excellent fits. This model and the IBA-1 models are also the only ones which provide a quadrupole moment of the 2_1^+ level as small as determined by measurement.[23,25] Thus, on all counts, these two simple models (i.e., IBA-1 and γ-soft) provide the best representation of our experimental results.

D. CE matrix elements

Finally, we present the results of employing the matrix elements not of any model, but those from the extensive Coulomb excitation experiments and analyses of Wu and Cline.[22] The neutron elastic scattering calculation at 4.55 MeV is then similar to that of the DDT model, the solid curve of Fig. 3. This is not as good a description as the γ-soft model. The inelastic scattering cross sections to the 2_1^+ level are shown as dashed curves in Fig. 6. Excitation of the 2_1^+ level is a little weak at 2.5 MeV, much like that of the DDT model. The worst calculations with the CE matrix elements are the total cross sections, shown as dashed curves in Figs. 2 and 7, where serious disagreement with measurements is found for $1.0 < E_n < 2.5$ MeV. Much of the problem with the CE calculations, as with the IBA-2 model, lies in the sign of the small matrix element directly coupling the ground state to the 2_2^+ level. If that one sign is changed, the fit to the total cross sections is much improved; however, the inelastic scattering cross sections to 2^+ levels are still low.

As a final remark we should note that none of the models tested really describes well the angular distributions for the second 2^+ level, either at 2.5 or 4.55 MeV incident energy. Scattering cross sections to the 2_1^+ and 4_1^+ levels are well represented, so we doubt that the weakness of the description of scattering to the second 2^+ level reflects

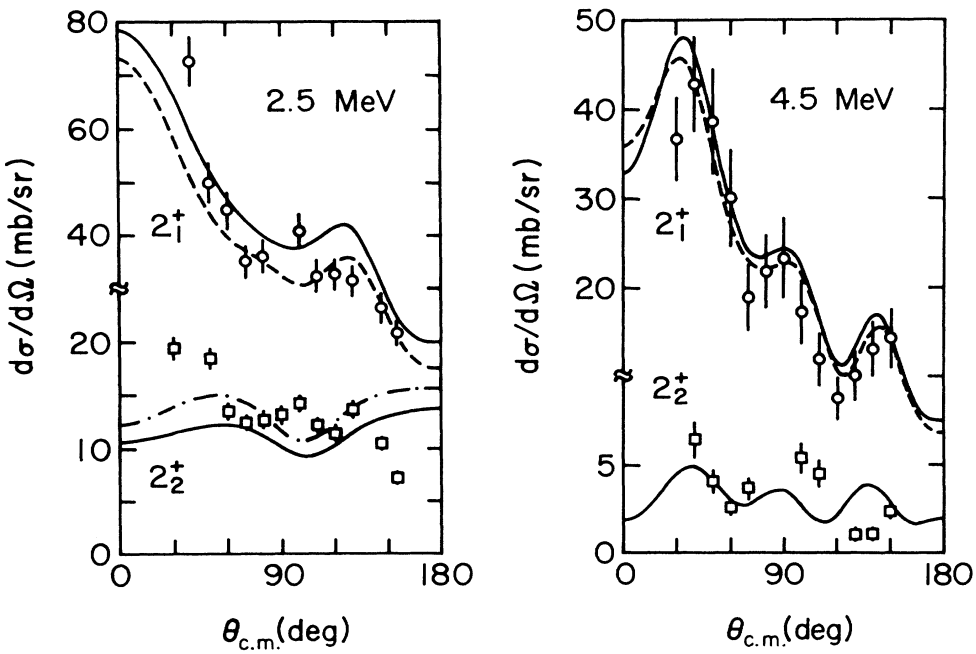

FIG. 6. Neutron scattering from the first two 2^+ levels at 2.5 and 4.55 MeV. The IBA-1 model calculations are plotted as solid curves, which also represent the γ-soft model *except* for the 2_2^+ level at 2.5 MeV. For that level the dotted-dashed curve would represent the γ-soft model. The dashed curves represent calculations using the CE reduced matrix elements.

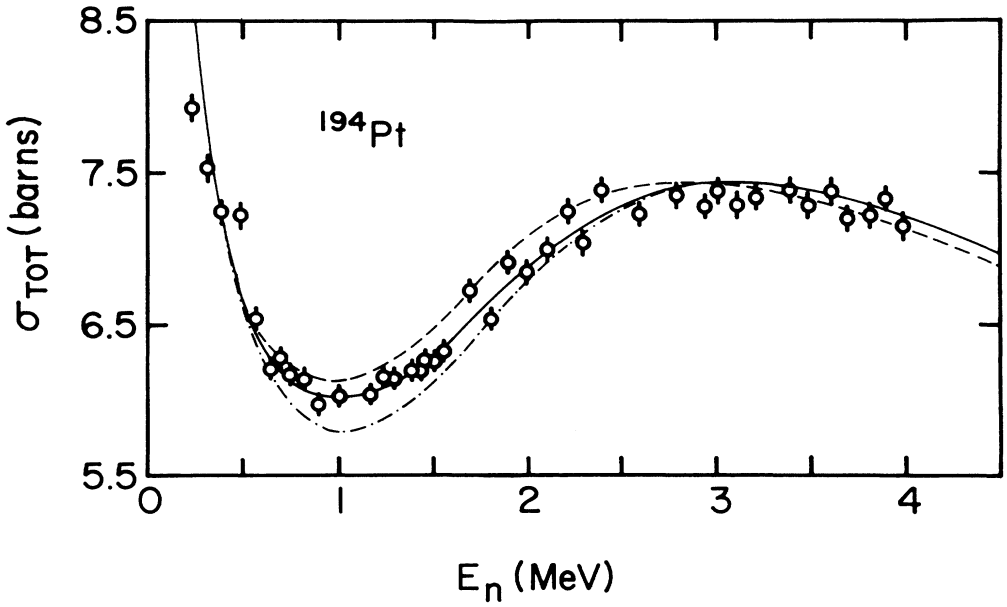

FIG. 7. Neutron total cross sections for ^{194}Pt are shown along with three model calculations. The solid curve is representative of either the IBA-1 or γ-soft model using the potential given in Table II. The dashed curve comes from calculations using the CE reduced matrix elements. The dotted-dashed curve is derived from the γ-soft model along with a real potential whose depth decreases linearly with neutron energy.

systematic model problems, or data problems. Something is missing in our description of that level, so that the angular distribution of the data is not well reproduced. Only the γ-soft model yields the correct magnitude of cross sections to that level.

E. Neutron scattering potentials

A significant surprise was the character of the scattering potentials required with realistic structure models. In fact, the potential parameter constraints were essentially the same for DDT, IBA-1, or γ-soft models. Our first approach to developing a scattering potential was to test local, linearly energy dependent potentials with fixed geometries, the normal procedure. However, we found that it was not possible to fit the neutron scattering data with such potentials. The dotted-dashed curve of Fig. 7, which results from using linearly energy dependent potentials, is obtained with any of the structure models which fit well differential elastic scattering cross sections (for example, the IBA-1 or γ-soft models).

The solid curves of Figs. 2 and 7 were calculated with the γ-soft model and a potential which was constant in strength below 4.6 MeV. To fit total cross sections from 4.6 to 30 MeV, the energy dependence was that indicated in Table II. The energy dependences of the potentials used with the DDT model, represented in Figs. 1 and 2, are also those of Table II. The energy dependence of potential parameters above 4.6 MeV were constrained not only by the three sets of total cross sections, but also through analysis of differential scattering cross sections measured at 8 MeV.[12]

The elastic scattering differential cross sections at 2.5 and 4.55 MeV required potentials whose real strengths were the same at both energies. Both analyses of differential scattering cross sections and analysis of the total cross sections required the same, constant real potential strength below 4.6 MeV. Furthermore, in order to provide a realistic fit to differential elastic scattering cross sections at 8 MeV,[12] we found it necessary to use a diffuseness much larger at 8 MeV than at 2.5 and 4.55 MeV. In Table II we present the potentials which describe our measurements for all of the successful structure models.

TABLE II. The nucleon scattering potential developed from neutron scattering data in conjunction with coupled-channels models as described in text. The quadrupole and hexadecapole coupling parameters β_2 and β_4 are also presented. The symbol V denotes real potential depth, W_D denotes surface absorptive depth, and V_{so} means real spin-orbit depth. All potential depths are specified in MeV. The radius parameters (R) and diffusenesses are given in fermis, R as a coefficient of $A^{1/3}$. The real potential diffuseness is nucleon energy dependent, as are the potential depths.

For incident energy $E<4.6$ MeV:	
$V=45.4$	$R/a=1.26/0.64$
$W_D=2.25+0.69E$	$R'/a'=1.28/0.47$
$V_{so}=6.30$	$R''/a''=1.12/0.47$
For incident energy $4.6<E<8$ MeV:	
$V=47.2-0.39E$	$R/a=1.26/(0.59+0.012E)$
$W_D=2.25+0.69E$	$R'/a'=1.28/0.47$
$V_{so}=6.30$	$R''/a''=1.12/0.47$
The deformation parameters:	
$\beta_2=-0.17\pm0.005$, $\beta_4=-0.04\pm0.005$	

The unusual energy dependences of the neutron scattering potential found here are just those reported earlier[28] for neutron scattering by ^{208}Pb. The authors of Ref. 28 attributed the nonlinear energy dependence of scattering strength, and the energy dependence of the real potential diffuseness, to an energy dependent effective nucleon mass, an effect particularly pronounced at energies close to the Fermi energy.[28] These same variable effective nucleon mass effects have been sought in neutron scattering from other nuclei with low neutron separation energies, near $A=90$. The tests for these mid-mass nuclei were negative; no evidence for nonlinear energy dependence of the scattering potential was required by the data.[29] It may be that we are seeing such effects in ^{194}Pt, and that they will only be evident in heavy nuclei. There is no question but that our data, both differential elastic and total scattering cross sections, do require a nearly constant real potential strength below 4.6 MeV.

F. Coupling strengths

Direct reaction cross sections determine coupling strengths, or deformation amplitudes. Excitation strengths associated with the scattering of different projectiles are compared to those from other observables, like electromagnetic decay probabilities, under the presumption that the collective properties controlling both types of strength are similar. In order to compare neutron coupling strengths with results obtained via electromagnetic excitation, we adopt the definitions of Ref. 5:

$$\beta_{n,n'}=\beta_2, \quad \delta_{n,n'}=\beta_{n,n'}R_t \ .$$

This allows us to make a geometry independent comparison of the deformations sensed by different probes. The deformations found from ^{194}Pt(n,n′) and electromagnetic decay are

$$\delta_{n,n'}=-1.239 \quad \text{(Ref. 12 and present work)} \ ,$$

$$\delta_{em}=-0.996 \quad \text{(Ref. 30)} \ .$$

The coupling strength required for neutron scattering, and possibly proton scattering,[6] is considerably stronger than that sensed by electromagnetic decay. The coupling required to describe neutron scattering from ^{194}Pt is well fixed, both at low and at high energies.[12] Lower values of β were used in test calculations to determine our sensitivity to this parameter. The dotted-dashed curve of Fig. 4 for the 2_1^+ level at 4.55 MeV incident energy demonstrates the effect of lowering β from -0.17 to -0.16. Neutron scattering from ^{194}Pt at 8 MeV also clearly requires[12] the value $\beta_2=-0.17$. The nuclear deformation sensed by proton scattering at 35 MeV is less certain, the uncertainty arising from the well known $W\beta$ ambiguity. Reference 6 contains a thorough examination of the deformation parameters required for scattering of both protons and neutrons from ^{194}Pt.

IV. SUMMARY

From our extensive coupled channels analyses based on various model assumptions, we must conclude that no single model completely describes the neutron scattering cross sections from ^{194}Pt. Certainly the γ-unstable or γ-soft models which leave the γ-band head almost decoupled from the ground state, characterize this nucleus best. The most successful models, IBA-1 and the γ-soft model of Leander, are quite consistent with the fact that the quadrupole moment of the first 2^+ level in ^{194}Pt is almost zero, and that this nucleus is also very near the O(6) limit of the IBA classification. Several models developed as improved versions for description of ^{194}Pt structure fail badly to describe scattering, notably the low energy total cross sections. These models include the ARM and recent IBA-2 description offered by Dieperink as an improvement over the 1980 IBA-2 description of Bijker and Dieperink. Two other models, the DDT and the first IBA-2 description, provided adequate fits to scattering, but not nearly as good as the simpler IBA-1 and γ-soft models. It is interesting that recent efforts to extend simple models, to provide more detailed fits to bound level properties, seem to move them away from better descriptions of scattering behavior. It is interesting also that γ-soft models, implying potential energy surfaces almost independent of γ, or degree of axial asymmetry, seem better suited to ^{194}Pt than γ-unstable models, which evoke potential energy surfaces with two distinct minima for different values of γ. A notable problem is describing scattering to the very weakly coupled γ-band head. The calculations for these cross sections seem to be out of phase with the data, both at 2.5 and 4.55 MeV. This probably reflects the sensitivity to mixing of strong collective levels with this very weak collective level.[31]

An unexpected energy dependence is required for the neutron scattering potential. We find that the real central potential saturates at low energies, so that below 4.6 MeV the strength is essentially constant. This is in contrast with the linear energy dependence usually found for scattering potentials. Also, the usual constant, energy independent scattering geometry is not adequate here.

The neutron differential scattering cross sections, measured at only three energies between 0 and 8 MeV, are not abundant enough to fix the functional form of the nonlinearity in the low energy behavior of the potential depth, or the form of the energy dependence of the diffuseness. However, both of these energy dependences are in the sense to correspond to variations of effective nucleon mass near the Fermi energy. Such effective mass variations were proposed to explain nonlinear potential strengths and energy dependent geometries in neutron scattering from ^{208}Pb; they were searched for without success in lighter nuclei. It may be that such effects are more evident in the heaviest nuclei. This extensive study illustrates the usefulness of neutron scattering at low incident energies as a sensitive probe of the dynamics of low lying nuclear excitations. The results complement well the information obtained from bound level decay studies.

ACKNOWLEDGMENTS

The authors acknowledge many discussions about the structural character of the shape-transitional nuclei with

Prof. J. L. Weil and Prof. S. W. Yates, as well as their generous assistance with data collection. One of us (J.P.D.) acknowledges with appreciation the support and encouragement afforded by the University of Kentucky while on leave from his home institution. The support of the National Science Foundation for this project through Grant PHY-84-03278 is gratefully acknowledged.

---

*Permanent address: Service de Physique et Techniques Nucléaires, Centre d'Etudes de Bruyères-le-Châtel, 91680, France.

†Present address: Department of Physics, Yarmouk University, Irbid, Jordan.

[1]M. T. McEllistrem, in *Neutron-Nucleus Collisions: A Probe of Nuclear Structure (Burr Oak State Park, Ohio, 1984),* edited by J. Rapaport, R. W. Finlay, S. M. Grimes, and F. S. Dietrich (AIP, New York, 1985) (AIP Conf. Proc. No. 124), p. 208.

[2]M. C. Mirzaa, J. P. Delaroche, J. L. Weil, J. Hanly, S. W. Yates, and M. T. McEllistrem, Phys. Rev. C **32**, 1488 (1985).

[3]J. L. Weil, in Proceedings of the Conference on Scientific and Industrial Applications of Small Accelerators [IEEE Trans. Nucl. Science **NS-28**, 1255 (1981)].

[4]J. Rapaport, Phys. Rep. **87**, 25 (1982).

[5]R. G. Kurup, R. W. Finlay, J. Rapaport, and J. P. Delaroche, Nucl. Phys. **A420**, 237 (1984).

[6]J. P. Delaroche, S. E. Hicks, and M. T. McEllistrem (unpublished).

[7]R. F. Casten and J. A. Cizewski, Nucl. Phys. **A309**, 477 (1978).

[8]W. P. Poenitz and J. F. Whalen, Argonne National Laboratory Report ANL/NDM-80, 1983.

[9]J. M. Peterson, A. Bratenahl, and J. P. Stoering, Phys. Rev. **120**, 521 (1960).

[10]A. J. Filo, S. W. Yates, D. F. Coope, J. L. Weil, and M. T. McEllistrem, Phys. Rev. C **23**, 1938 (1981).

[11]R. E. Shamu, Ch. Lagrange, E. M. Bernstein, J. J. Ramirez, T. Tamura, and C. Y. Wong, Phys. Lett. **61B**, 29 (1976).

[12]T. B. Clegg, M. T. McEllistrem, G. Haouat, J. P. Delaroche, S. E. Hicks, Ch. Lagrange, G. R. Shen, and J. Chardine (unpublished).

[13]F. D. McDaniels, J. D. Brandenberger, G. P. Glasgow, and H. G. Leighton, Phys. Rev. C **10**, 1987 (1974); D. F. Coope, S. N. Tripathi, M. C. Schell, J. L. Weil, and M. T. McEllistream, *ibid.* **16**, 2223 (1977).

[14]Joseph L. Cochran, M.Sc. thesis, University of Kentucky, 1974 (unpublished).

[15]Steven E. Hicks, Ph.D. Dissertation, University of Kentucky, 1987 (unpublished).

[16]A. Bratenahl, J. M. Peterson, and J. P. Stoering, Phys. Rev. **110**, 927 (1958).

[17]F. H. Frohner, Atomic Energy Commission Research and Development Report Number GA-8380, 1968.

[18]J. Raynal, ECIS79 (unpublished); J. Raynal, *Computing as a Language of Physics* (IAEA, Vienna, 1972); *The Structure of Nuclei* (IAEA, Vienna, 1972), p. 75; J. Raynal, Phys. Rev. C **23**, 2571 (1981).

[19]R. Bijker, A. E. L. Dieperink, O. Scholten, and R. E. Spanhoff, Nucl. Phys. **A344**, 207 (1980); R. Bijker, private communication.

[20]A. E. L. Dieperink, in *Collective Bands in Nuclei,* edited by D. Wilkinson (Pergamon, New York, 1983), p. 121.

[21]K. Kumar, Phys. Lett. **29B**, 25 (1969).

[22]Ching-Yen Wu, Ph.D. dissertation, The University of Rochester, 1983 (unpublished); D. Cline, Annu. Rev. Nucl. Part. Sci. **36**, 683 (1986); D. Cline, private communication.

[23]C. Y. Chen, J. X. Saladin, and Abdul A. Hussein, Phys. Rev. C **28**, 1570 (1983).

[24]G. Y. Gyapong, R. H. Spear, M. T. Esat, M. P. Fewell, A. M. Baxter, and S. M. Burnett, Nucl. Phys. **A458**, 165 (1986).

[25]M. V. Hoehn, E. B. Shera, H. D. Wohlfahrt, Y. Yamazaki, and R. M. Steffen, Bull. Am. Phys. Soc. **24**, 53 (1979).

[26]P. T. Deason, C. H. King, R. M. Ronningen, T. L. Khoo, F. M. Bernthal, and J. A. Nolen, Phys. Rev. C **23**, 1414 (1981); P. T. Deason, Jr., Ph.D. dissertation, Michigan State University, 1979 (unpublished).

[27]G. Leander, Nucl. Phys. **A273**, 286 (1976).

[28]See R. W. Finlay, J. R. M. Annand, J. S. Petler, F. S. Dietrich, in Ref. 1, p. 322; Phys. Lett. **155B**, 313 (1985).

[29]A. B. Smith, P. T. Guenther, and R. D. Lawson, Nucl. Phys. **A455**, 344 (1986); A. B. Smith, P. T. Guenther, and R. D. Lawson, Argonne National Laboratory Report ANL/NDM-91, 1985.

[30]S. Raman, C. H. Malarkey, W. T. Milner, C. W. Nestor, Jr., and P. H. Stelson, At. Data Nucl. Data Tables **36**, 1 (1987).

[31]J. P. Delaroche and F. S. Dietrich, Phys. Rev. C **35**, 942 (1987).